TECHNICAL PAPER

Design and implementation of an electrode feed rate control system in the electrochemical drilling process

Hacı Bekir Özerkan[1] · Can Çoğun[2]

Abstract

The interelectrode gap distance control is essential for preventing short circuit and spark discharge occurrences in the machining gap and ensuring a constant distance between the tool electrode (shortly electrode) and the workpiece throughout the electrochemical drilling (ECD) process. In this study, a gap distance control system was designed and implemented in the constructed ECD machine tool. The gap distance control strategy was based on the machining current's discrete measurement (in microsecond intervals) and changing the gap distance according to a set current value by feeding the electrode towards the workpiece or retracting it during the ECD process. The small diameter deep hole ECD experiments were conducted using 0.5 mm diameter side insulated tubular rotational electrodes with through-hole electrolyte flushing to drill Hadfield and AISI 1040 steels. The experimental results demonstrated the success of the developed control system in ECD operations yielding uniform hole geometries and smooth hole surfaces. The use of the control system eliminated the undesirable formations of spark discharges and short circuit pulses.

Keywords Electrochemical drilling · Electrode feed rate control · Control software · Tubular rotational electrode

1 Introduction

Electrochemical drilling (ECD) is a nontraditional machining process that removes workpiece atoms in ionic form by anodic dissolution (electrolysis) mechanism. Electrolysis occurs when an electric current passes between the electrode and workpiece immersed in an electrolyte solution. The ECD offers advantages like higher machining rate, zero electrode wear, no burrs, better surface quality and machinability of a broader range of electrically conductive materials (workpieces) with good dimensional accuracy [1]. Also ECM is a process that requires detailed knowledge of corrosion, passivation, interface kinetics, materials science, crystallography, fluids and electronics [2]. It is a contactless machining method, it is suitable for difficult-to-cut materials, regardless

✉ Hacı Bekir Özerkan
   ozerkan@gazi.edu.tr

1   Department of Mechanical Engineering, Engineering
    Faculty, Gazi University, Ankara, Turkey

2   Department of Mechatronics Engineering, Engineering
    Faculty, Çankaya University, Ankara, Turkey

of their hardness and strength [3]. In recent years, there have been some major areas of research on ECM, here the purpose is to improve the dissolution conditions in the interelectrode gap and keep small, stable gaps to achieve higher machining accuracy, good surface quality, and better process stability [4]. It is well known that the electrochemical machining rate reaches a state of relative equilibrium material removal rate (MRR) after a transition stage and this relative equilibrium MRR is higher than the feed rate, resulting in a linear increase in IEG [5]. Therefore, an accurate tool motion strategy for material removal rate (MRR) and interelectrode spacing (IEG) variations at different machining parameters is important for shape and dimensional accuracy [6]. The ECD process is also applied to micro applications to manufacture ultra-precision shapes [7, 8]. Manufacturing micro features with high dimensional accuracy depends on close control of gap distance. However, the close control of the gap distance is complicated due to the continuous change of machining medium characteristics, such as current density, electric field strength, electrolyte salt concentration, flushing pressure, power supply pulse characteristics, and the electrical conductivity of the environment, which affect the machining performance (i.e., the workpiece removal rate (WRR), dimensional accuracy and surface texture) directly

[9]. Therefore, it is crucial to monitor the gap distance variation during ECM to precisely control dimensional accuracy by considering the processing variables [10]. Rajurkar et al. [11] developed a model to forecast the minimum gap distance and found that a shorter pulse on time would allow a smaller gap distance without short circuits. For this purpose, real-time current changes at the gap have been used for predicting the gap distance with an accuracy of 0.002 mm in an experimental pulse electrochemical machining (ECM) system, which includes a transistorized pulse generator and a computer-based data acquisition system. The developed data acquisition system could sample and save the signals at a rate of 1 μs. They reported a linear correlation between the signal variance of the filtered current and the gap distance within the gap distance range of 0.1–0.2 mm. Bhattacharyya et al. [12] designed a microprocessor-based automatic electrode motion control unit to achieve a stable machining performance in ECM. The unit enabled short circuit prevention, spark detection, and auto-tripping by a closed-loop control electronic circuitry with a microprocessor for achieving the desired electrode feed rate (FR) settings and constant machining current. The feedback signal consisted of input AC variation due to the machining conditions, such as fluctuation in the voltage drop, which is monitored by the three current transformers across the gap distance [12, 13]. Lu et al. study [14], the gap distance was measured by mounting a 6-axis force sensor to the electrode. It was found that the force measured on the electrode increased with the decrease of the gap and there was a linear relationship between the gap distance and force variation. It was also emphasized that activation of the electrode disrupted this relationship due to processing flow, gas bubbles and other factors. In their control strategy, it was necessary to initially feed the electrode at minimal speeds to obtain dimensional accuracy and prevent electrode-workpiece contact [15]. Clifton et al. [16] introduced ultrasound for gap distance measurement in ECM. The experimental setup consisted of an ultrasonic receiver and transmitter transducer and a CLF4 piezoelectric/Perspex delay-line system (15 MHz frequency) positioned under the workpiece. They used the gap distance measurements to quantify the degree of departure from ideal behavior in Inconel 718 alloy machining with chloride electrolyte. They have shown that the measurement of the gap distance has been very effective in displaying the machining profile and dimensional change in 2-D. The NC-ECCEM (numerical control-electrochemical contour evolution machining) process combines the advantages of ECM and NC techniques providing machinings with high dimensional accuracy and removing small-to-medium amounts of material from the workpiece [17–19]. In Jiawen et al. study [20] on NC-ECCEM, the feed of the rotary electrode controlled by the NC system in which a stepped-motor drives each axis made the WRR either bigger or smaller with achieving excellent

processing stability and high dimensional accuracy. In the study, an integral wheel with twisted blades workpiece was machined by a simple non-profiled electrode moving along a contour trace. In Yong et al. study [21], an experimental setup has been constructed containing gap control following the current jump-up signals. The electrode gap control within a few 10 μm was achieved by measuring the current between electrode and workpiece and feedbacking it to the ADC-PC-power amplifier. In Kurita et al. study [22], an electrochemical micro-machining system, which consisted of a PC, a triaxial DC pulse motor and a piezo-transducer (PZT), enabled the high-speed movement of the tool with 0.0156 mm/pulse movement resolution in the z-direction. The PC in the system can set the processing conditions, the actuators' operating control, and the power supply data. In Labib et al. study [23], the voltage, current, flushing flow rate, electrolyte conductivity and electrolyte temperature input variables have been identified and measured to monitor and control the ECD process. Two fuzzy logic controllers consisting of two inputs and one output were created in the Mathworks-Matlab Fuzzy Logic Toolbox to monitor and control the electrode FR (− 1.0 to 1.0 mm/min) and flow rate (0–11 l/min) of the process for input current settings between 0 and 50 A. In Liu et al. study [24] in which the gap distance control was performed using the Hall effect sensor, it was tried to keep the gap distance constant by measuring the current continuously during processing. The distance between the sample and the electrode compared to the originally determined stand of distance using the signals from the voltage and current sensor. Thus, a certain amount of forward or backward movement of the tool according to the error values was realized by using a linear ball screw mechanism with a servo stepper motor. Within the scope of the study, the gap between the workpiece and the tool electrode was achieved between 0.01 and 0.1 mm.

It is known that electrochemical reaction products formed during small diameter deep hole drilling should be removed effectively from the front and side (lateral) gaps of the hole. Otherwise, the current distribution disperses nonuniformly, limiting the dimensional precision and the machining stability of the drilling operation. In the small diameter deep hole ECD process, the instantaneous electrical conductivity in the machining gap, which depends on the instantaneous salt concentration of the electrolyte, the medium temperature, the amount of dissolved metal ions, the variation of workpiece material properties with the depth of the hole, could only be determined by the measurement of the current passes from the machining medium. In this study, the current flow from the machining gap was kept constant (a preset setting) by feeding and retracting the electrode with a servomotor controlled by a microprocessor and the developed software to keep the gap distance constant. High depth-to-diameter ratio hole drilling experiments were conducted to understand

the operational success of the developed control system. Accordingly, this paper presents the operating principles of the current feedback control system, its components, the developed control software, and the results of the drilling experiments that reflect the control system's performance.

2 The ECD experimental setup and gap distance control system

2.1 The ECD machine tool

In this study, a desktop ECD unit consisting of a machine body, an electronic control unit and software, DC power supplies, an electrolyte supply and a pressurization unit, a pressure head and a tool holder system was designed and fabricated (Fig. 1). The electrolyte was filled into the plexiglass electrolyte tank. A piston pump was used for the pressurization of the electrolyte. The electrode was fed or retracted using a trapezoidal screw, which was rotated by a DC motor mounted to the pressure head (Fig. 2). The pressure also applied a high-pressure electrolyte (max. 10 MPa) through the electrode. The electrode was mounted to the pressure head using a holder. The electrode passed through a ceramic guide to prevent vibration and lateral movement
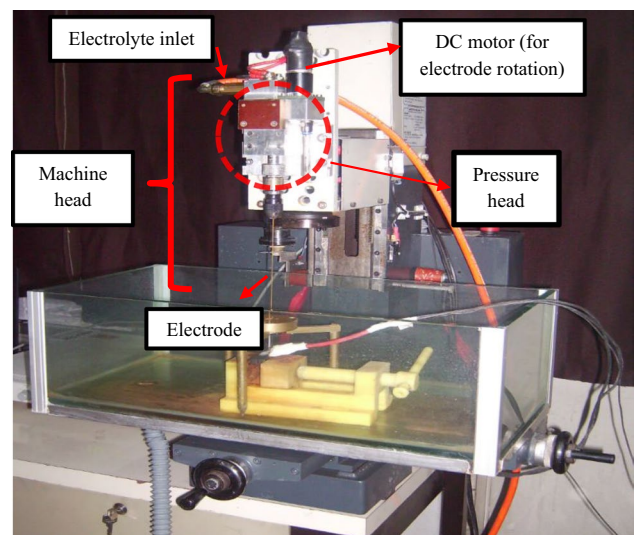

Fig. 2 The ECD machine body

during the ECD process (Fig. 3). Another DC motor provided the rotational motion of the electrode. The DC motors were controlled by MIP (Microsoft Information Protection) 10 control unit (Fig. 4). The structural and mechanical details of the built ECD machine, including the technical
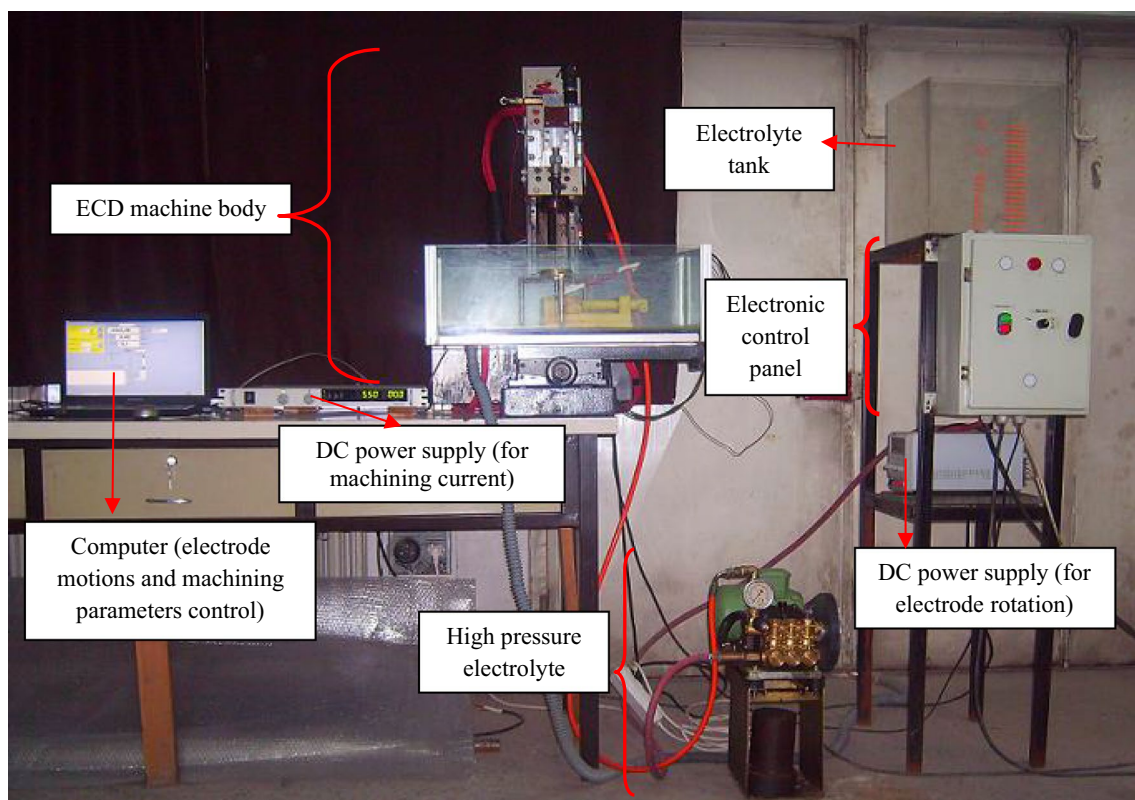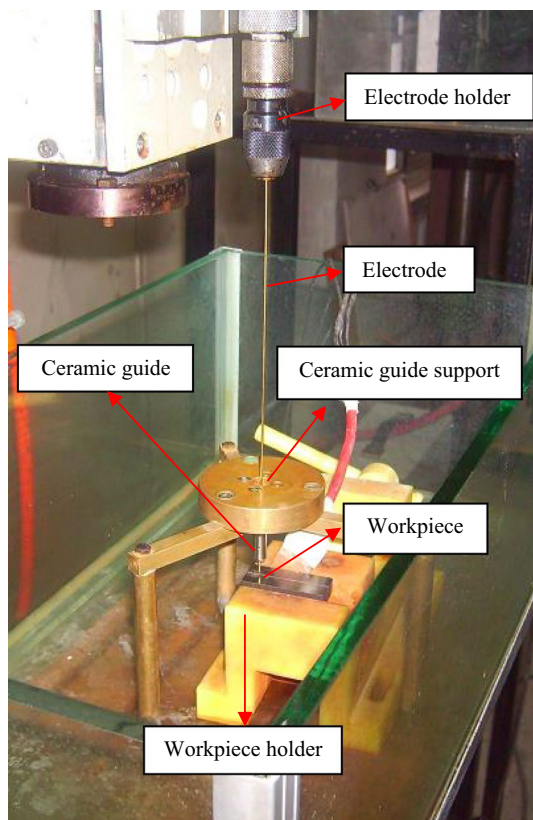

Fig. 1 The experimental ECD setup
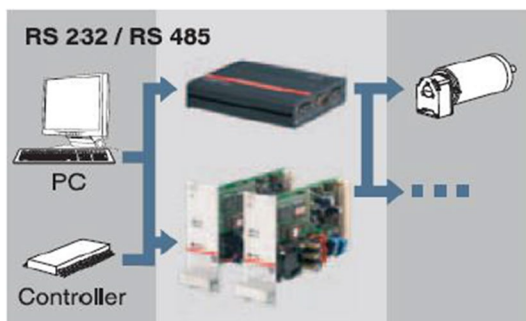
Fig. 3 Mounting of the tubular tool

Fig. 4 The MIP control mode of DC motors

specifications and accuracy values, were given another publication by the authors [25].

2.2 The gap distance control system

The DC motor rotation speed information, which depends on the discrete measurement of current over the workpiece and electrode (I_m), was received from a program written in Delphi language. A current sensor was used to measure the I_m. The analog I_m measurement was discretized using an ADC and sent to the computer control software through the current assessment module of the controller card (Fig. 5). After data processing, the control information (the current electrode position, FR, gap distance) was sent to the servomotor with the control card and MIP10.

Although the designed and implemented control system enabled the user to select the constant FR or constant current control strategy option, the constant current is advisable to have a higher WRR and better dimensional and geometric tolerances for the workpiece materials not tested before. The constant FR strategy option could be selected for drilling operations experienced before. Figure 6 shows the constant current control strategy used in this study. Before the start of the machining, the constant current value (I_s) was set by adjusting the programmable main DC power supply (0–7.5 V, 0–140 A (max. 1200 W)). Initially, the electrode approached the workpiece using the "touch module" of control software. After the first touch, the electrode was retracted by 1 mm. In this study, the DC motor provided FR in the 0–1 mm/s range with a 0.0001 mm/s increment. After the machining started, the I_m was measured and compared with the I_s. If there was a difference between them, the I_m value was sent to the MIP through the integrated control card. The MIP sent the electrode feed motor commands to feed or retract to maintain a constant gap distance. The electrode's retraction rate (RR) was set as two times the instantaneous FR to eliminate even the small risk of short circuit occurrences. In calculating instantaneous FR and RR, the instantaneous value of the $I_m - I_s$ was used to keep the rates low (or high) when the I_m-I_s difference was small (or high) to maintain a stable machining regime. If $I_m > I_s$ (i.e., the instantaneous gap is narrower than the stable machining regime gap), the electrode was retracted at a rate equal to $-2 \times (I_m - I_s) \times$ RF, and if $I_m < I_s$, the electrode was fed with a rate equal to $-1 \times (I_m - I_s)$ x RF. The vectorial signs of feed and retraction rate are always + and − , respectively. Here, RF is the rate factor that could be set between 6 and 9 µm/s for the experimental settings used in this study. The RF selection depends on the workpiece material characteristics (especially its anodic dissolution rate), hole dimensional and geometric tolerances, hole drilling time and electrode motion stability. In lower RF settings, the lower FR (i.e., longer electrolysis time at the same location) resulted in a larger diameter hole, poor dimensional and geometric tolerances and longer drilling time. In turn, the higher RF values were preferred in the ECD of Hadfield steel to reduce the drilling time since it had a lower electrolytic dissolution rate than the AISI 1040 steel. The RF values above 10 µm/s caused undesired electrode up and down oscillations during ECD.
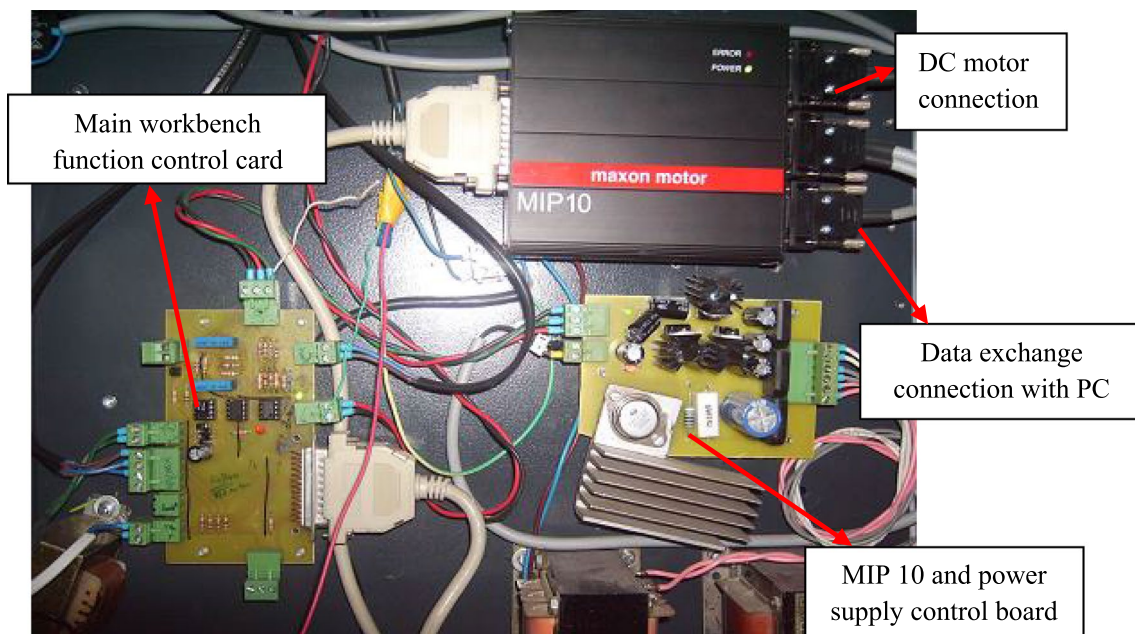
Fig. 5 The control board (the data collection, transfer and recording system)
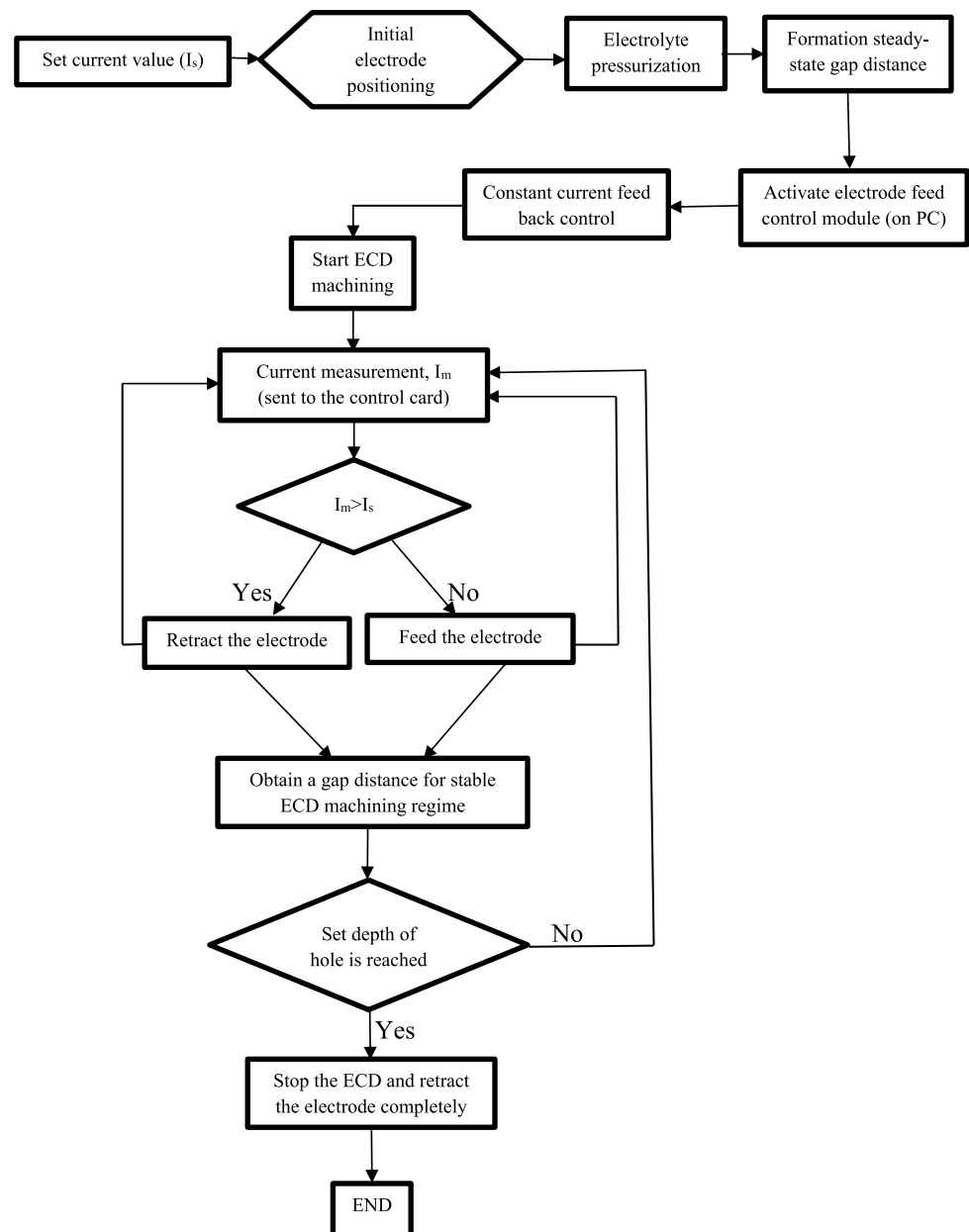
2.3 The control program menus

The following menus are developed to control the ECD machine tool.

(a) The "general settings menu" (Fig. 7) includes; (i) the data cable connection to the computer's USB port (the data exchange between the computer software and the MIP control unit), (ii) the communication speed of the computer, the MIP and the current sensor, (iii) the connection check of MIP, (iv) the torque control of the servo motor, (v) electrode feed acceleration and deceleration settings.

(b) The "touch function menu" sets the electrode's approach velocity (µm/s) to the workpiece and the distance between the electrode and the workpiece (µm) before machining.

(c) The "manual control menu" activates the manual control in case of excessive short circuit formations or electrode-workpiece stickings during ECD.

(d) The "constant FR machining menu" sets the constant FR and the machining depth. The interface also enables the user to calculate the electrolytic dissolution rates of metals by the formula to find the approximate FR.

(e) The "constant current machining menu" (Fig. 8) sets the constant machining current (I_s), the machining depth and rate factor (RF). It also shows the FR, instantaneous current, and electrode depth during machining.

3 The experimental procedure

The ECD experiments were carried out by using the developed experimental setup. Due to their high rigidity and electrical conductivity, brass hollow electrodes with 0.5 mm outer diameter and 0.18 mm hole diameter were used. Only the tool's front surface (tip) was used for anodization since the external cylindrical surface of the brass tube electrodes was insulated. So, even though the drilling depth has increased, no current change was observed. The AISI 1040 steel and Hadfield steel were used as workpiece materials. The main reasons for this choice were that these materials were good electric conductive and difficult to machine by conventional chip removal processes due to their high hardness. Ninety-six experiments were conducted using rotating and non-rotating electrodes for ECD of the Hadfield steel and AISI 1040 steel workpieces at the machining settings combinations given in Table 1. The authors presented the detailed experimental procedure and the results in another study [24]. The measured instantaneous electrode tip position (i.e., depth of hole), FR, I_m (measured current), and t_m (machining time) values were monitored and recorded in an xls file every 0.5 s. When the electrode was approached about 50–80 µm above the workpiece surface, the I_m reached nearly the steady-state (I_s) value.

Fig. 6 The constant current feedback control strategy

Set current value (I_s) → Initial electrode positioning → Electrolyte pressurization → Formation steady-state gap distance

Constant current feed back control ← Activate electrode feed control module (on PC)

Start ECD machining

Current measurement, I_m (sent to the control card)

$I_m > I_s$

Yes → Retract the electrode   No → Feed the electrode

Obtain a gap distance for stable ECD machining regime

Set depth of hole is reached — No

Yes

Stop the ECD and retract the electrode completely

END

4 Experimental results and discussion

Figure 9 shows the variation of I_m with t_m for drilling the sample holes with electrode rotation. The drilling experiments were completed in 1050–2200 s depending on the machining settings and workpiece materials. In the experiments, the I_m values were nearly zero in the operation's first 50–200 s (i.e., during the electrode approach to the workpiece). When the electrode reached a distance suitable for the start of anodic dissolution, the I_m approached its set value (I_s). The I_s was set below 1 A in all drilling experiments to have precision holes with better geometrical and dimensional tolerances. The I_m depended on the instantaneous gap conditions (the electrolyte temperature, salt

concentration, electrolyte flow characteristics in the front and side gaps, work material homogeneity, the effectiveness of interelectrode gap flushing from debris, and gas bubbles). The zigzag behavior of I_m during drilling (Fig. 9) was due to the electrode's up and down movements to keep the I_m close to the I_s. During the drilling experiments, the developed control strategy and the constructed circuits prevented spark discharges and short circuits. The shorter ECD machining time (about 5–9%) to drill a hole with the developed control strategy than the case without the control strategy was attributed to fewer spark discharges and short circuits during the experiments. The rare machining instabilities generally occurred at the end of the experiments due to difficult flushing conditions at the bottom of the holes. The graphs
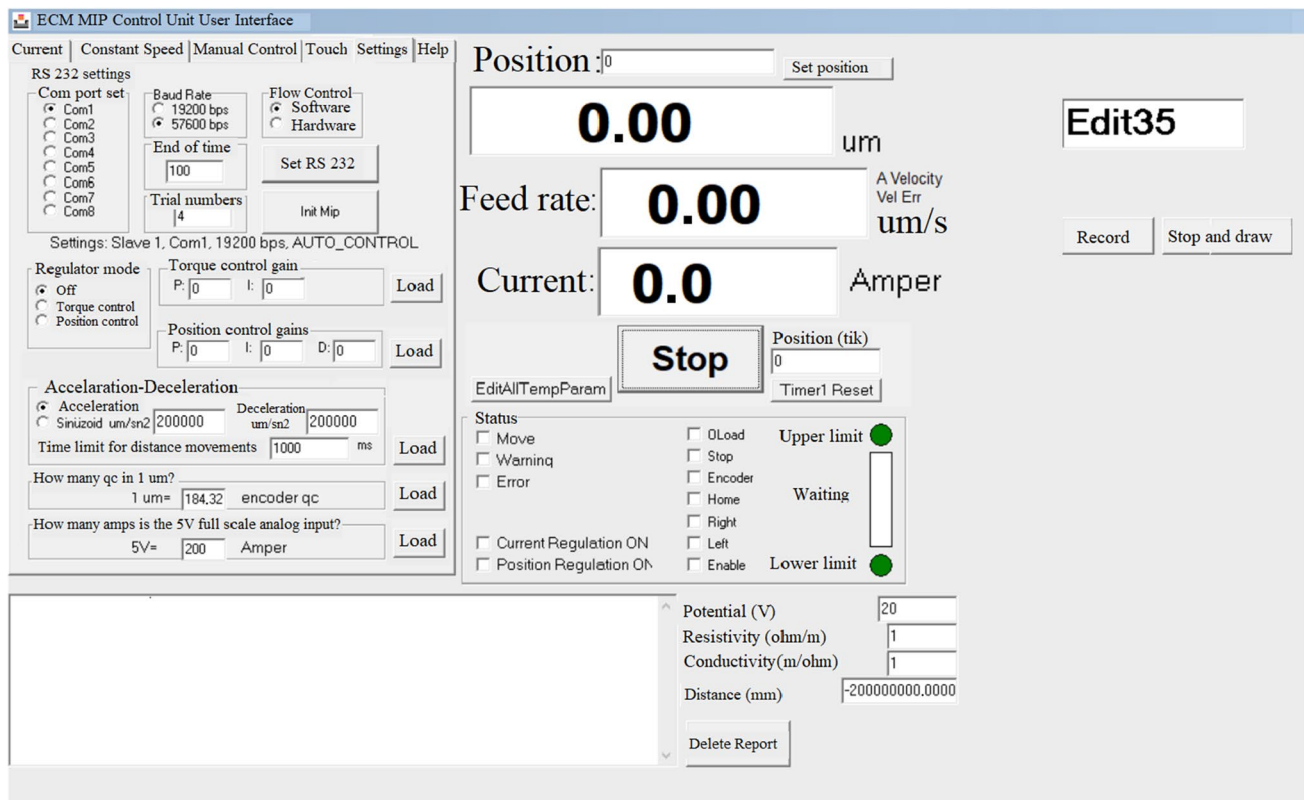
Fig. 7 The electrode motion control user menu

revealed that the control strategy successfully maintained the steady-state gap conditions by changing the current (I_m) in 0.1–0.2 A. The slight I_m variations throughout the process resulted in uniform electrochemical reactions at the interelectrode gap, yielding uniform hole geometries and smooth hole surfaces (Figs. 10, 11). Some dimensional inaccuracies and surface defects identified in the holes were attributed to the inhomogeneous distribution of elements and phases of the workpieces, causing dissolution of structurally and compositionally different material regions at different rates. Moreover, coarse particulates of decomposed electrolyte and small ionic workpiece material residues might block the side gap and reduce the current density locally, causing different anodic dissolution properties. So, hole diameters slightly changed along with the hole depth because of the variations in current density during the drilling operation.

In drilling experiments, the WRR increased with increasing machining voltage V, electrolyte concentration C, electrolyte injection pressure P and electrode rotational speed n. The holes have been drilled in a short time since the higher WRR values were obtained in AISI 1040 steel specimens due to their high anodic dissolution characteristics. The rare clogging of the side gap has been observed in the Hadfield steel workpiece. The average side gap (overcut) increased with increasing n and decreased with increasing V and C for both workpieces. Geometrically and dimensionally precise holes were obtained in the ECD of AISI 1040 steel.

This study revealed that the performance of the designed and implemented control system significantly contributed to the success of the small diameter deep hole ECD process. The electrode rotation, which enhanced the removal of the processing debris from the gap, has secondary importance in the success of the processes.

5 Conclusion

A gap distance control system based on the machining current's (I_m) measurement and changing the gap distance according to a set current value (I_s) by feeding or retracting the electrode during the ECD process was designed and implemented.

The FR and RR were found from $1 \times (I_m - I_s) \times RF$ and $-2 \times (I_m - I_s) \times RF$ formulations. The use of I_m-I_s difference in the calculation of instantaneous FR and RR stabilized the machining regime by minimizing the feed rate of the electrode, especially at direction changes. The FR in the 0–1 mm/s range and the RR as two times the instantaneous FR were suitable settings for a stable machining regime. The low RF settings yielded low FRs, which resulted in holes
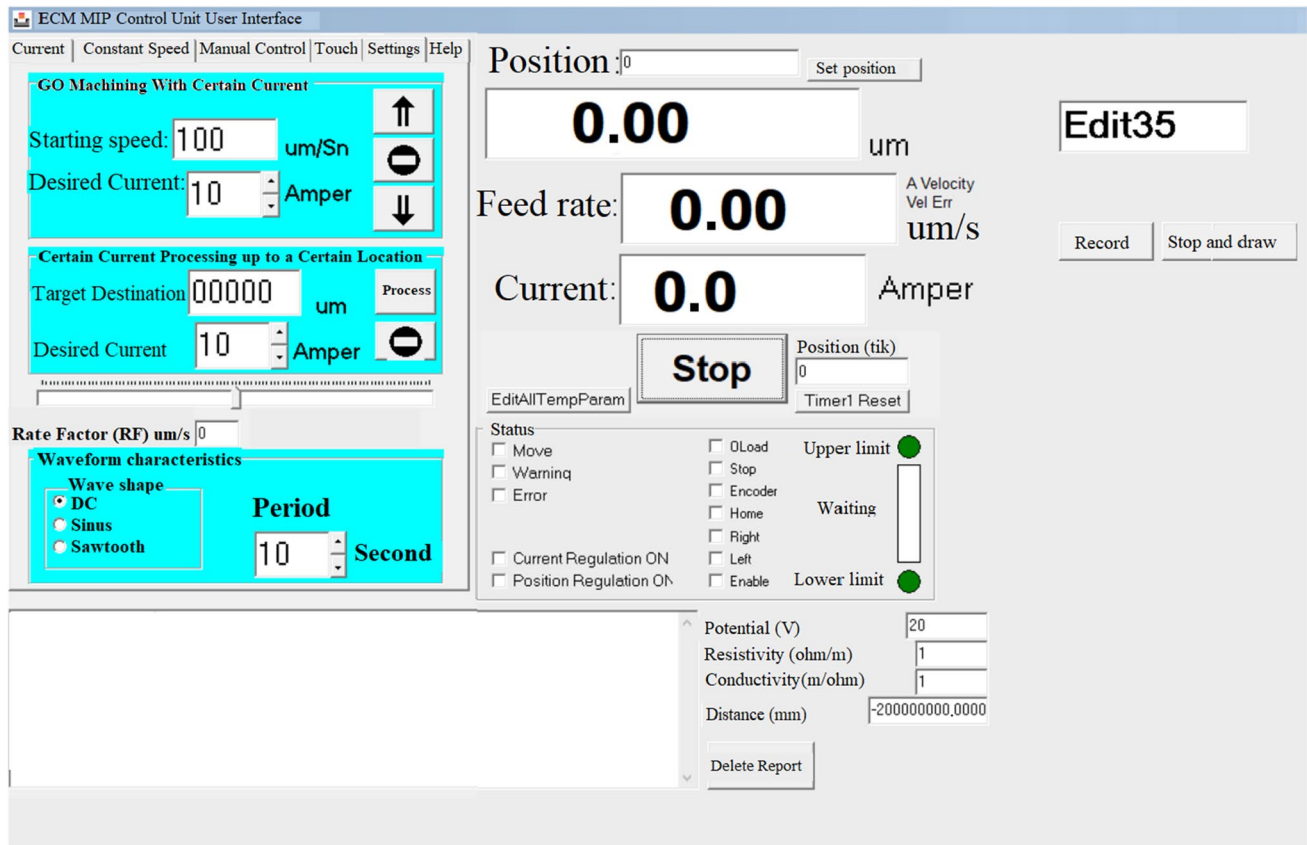
Fig. 8 The constant current machining user menu

Parameters	Settings
Workpiece	Hadfield and AISI 1040 steel
Electrode	Tubular brass, $D = 0.5$ mm, $d = 0.18$ mm, L = 300 mm
Drilling depth [mm]	8 (through-hole)
Machining voltage, V [Volt]	4.5–5.5–6.5
Initial gap distance [μm]	600
Electrolyte	NaCl solution (in water)
Electrolyte concentration, C [g/l]	100, 125, 150
Electrolyte application type	Injection through tubular electrode hole
Electrolyte Injection pressure, P [MPa]	2, 4
Electrode rotational speed, n [rpm]	200, 400
Polarity	Electrode (−), workpiece (+)

Table 1 The experimental ECD parameters [24]

with large diameters, poor dimensional and geometric tolerances, and long drilling time.

The $I_s < 1$ A experiments yielded precision holes with good geometrical and dimensional tolerances. The control strategy successfully maintained the steady-state gap conditions by changing the current to about 0.1–0.2 A. The holes in AISI 1040 steel have been drilled shorter than the 1040 steel since the 1040 steel has a higher anodic dissolution characteristic. Geometrically and dimensionally, more precise holes were obtained in the ECD of AISI 1040 steel than in Hadfield steel.

The performance of the designed and implemented current feedback control system significantly contributed to the success of the small diameter deep hole ECD process. The control strategy is advisable to have a higher workpiece removal rate and better dimensional and geometric

Fig. 9 Variation of I_m with t_m for sample holes; **a** Hadfield steel, exp. no: 65 (7.5 V, 125 g/l, 21 min), **b** Hadfield steel, exp. no: 70 (7.5 V, 150 g/l, 20.5 min), **c** AISI 1040 steel, exp. no: 2 (4.5 V, 100 g/l, 34 min), **d** AISI 1040 steel, exp. no: 50 (7.5 V, 100 g/l, 16 min)
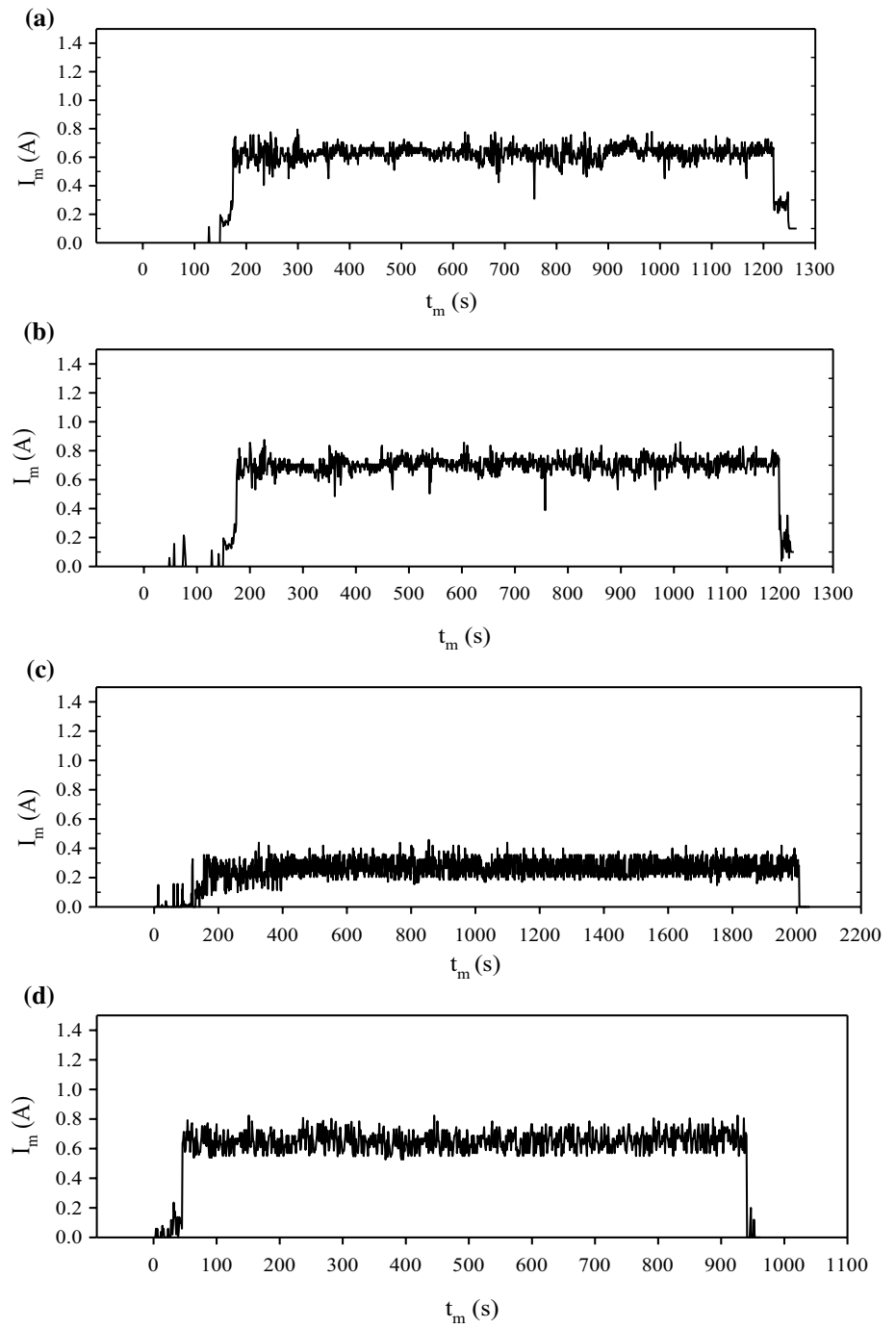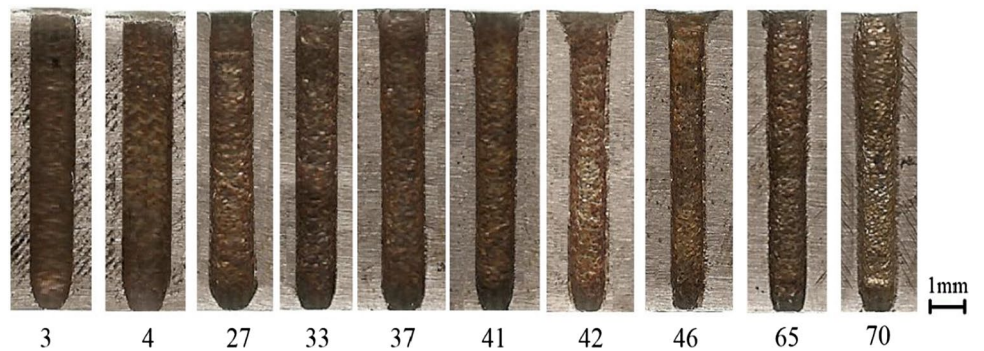

Fig. 10 The cross-sectional views of sample holes drilled to Hadfield steel workpiece (the numbers indicate the exp. no)
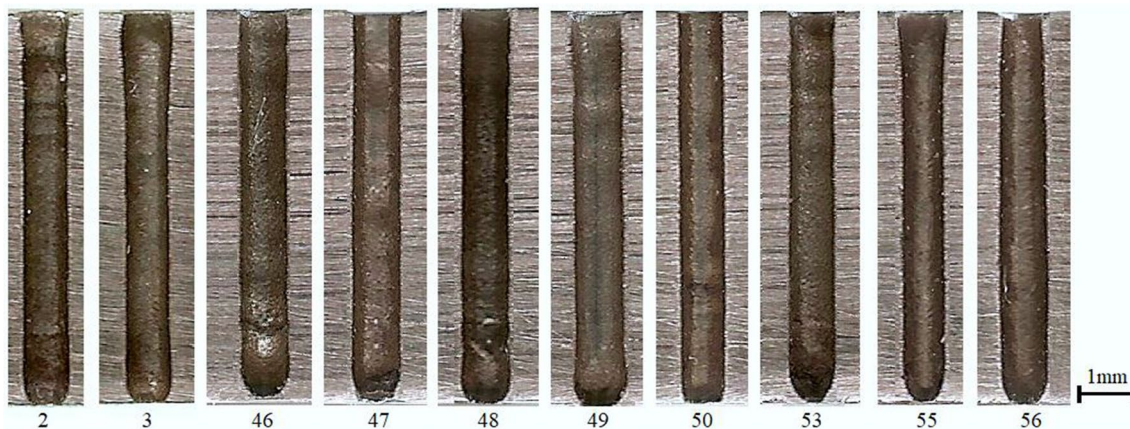
Fig. 11 The cross-sectional views of representative holes drilled to the AISI 1040 steel workpiece (the numbers indicate the exp. no)

tolerances. The electrode rotation, which enhanced the removal of the processing debris from the gap, improved the steel's electrochemical machinability. The system prevented spark discharges and short circuits during the experiments and decreased the ECD machining time by 5–9%.

References

1. Lohrengel MM, Rataj KP, Münninghoff T (2016) Electrochemical Machining mechanisms of anodic dissolution. Electrochim Acta 201:348–353. https://doi.org/10.1016/j.electacta.2015.12.219

2. Zhengyang XU, Yudi WANG (2019) Electrochemical machining of complex components of aero-engines: developments, trends, and technological advances. Chin J Aeronaut 34(2):28–53. https://doi.org/10.1016/j.cja.2019.09.016

3. Cao W, Wang D, Zhu D (2020) Modeling and experimental validation of interelectrode gap in counter-rotating electrochemical machining. Int J Mech Sci 187:105920. https://doi.org/10.1016/j.ijmecsci.2020.105920

4. Bhattacharyya B (2015) Electrochemical micromachining for nanofabrication, MEMS and nanotechnology. William Andrew. https://doi.org/10.1016/C2014-0-00027-5

5. Tsuboi R, Yamamoto M (2009) Modeling and applications of electrochemical machining process. ASME Int Mech Eng Congress Expos 43772:377–384. https://doi.org/10.1115/IMECE2009-12552

6. Davydov AD, Volgin VM, Lyubimov VV (2004) Electrochemical machining of metals: fundamentals of electrochemical shaping. Russ J Electrochem 40(12):1230–1265. https://doi.org/10.1007/s11175-005-0045-8

7. Saxena KK, Qian J, Reynaerts D (2018) A review on process capabilities of electrochemical micromachining and its hybrid variants. Int J Mach Tools Manuf 127:28–56. https://doi.org/10.1016/j.ijmachtools.2018.01.004

8. Rajurkar KP, Zhu D, McGeough JA, Kokaz J, De Silva A (1999) New development in electrochemical machining. Ann CIRP 48(2):567–579. https://doi.org/10.1016/S0007-8506(07)63235-1

9. Bhattacharyya B, Munda J (2003) Experimental investigation on the influence of electrochemical machining parameters on machining rate and accuracy in micromachining domain. Int J Mach Tools Manuf 43(13):1301–1310. https://doi.org/10.1016/S0890-6955(03)00161-5

10. Rajurkar KP, Sundaram MM, Malshe AP (2013) Review of electrochemical and electro-discharge machining. Procedia CIRP 6:13–26. https://doi.org/10.1007/s11175-005-0045-8

11. Rajurkar KP, Wei B, Kozak J, McGeough JA (1995) Modelling and monitoring lnterelectrode gap in pulse electrochemical machining. Ann ClRP. https://doi.org/10.1016/S0007-8506(07)62301-4

12. Sorkhel SK, Bhattacharyya B, Rudra C (1990) Control of machining rate and surface characteristics in constant current electrochemical machining. In: Proc. 1st int. conf. new manufacturing technology, Chiba, pp 597–601

13. Bhattacharya B, Sorkhel SK (1999) Investigation for controlled electrochemical machining through response surface methodology based approach. J Mat Proc Tech 86:200–207. https://doi.org/10.1016/S0924-0136(98)00311-2

14. Lu Y, Liu K, Zhao D (2011) Experimental investigation on monitoring interelectrode gap of ECM with six-axis force sensor. Int J Adv Manuf Tech 55:565–572. https://doi.org/10.1007/S00170-010-3105-5

15. Dengyong WANG, Jinzheng LI, Bin HE, Di ZHU (2019) Analysis and control of inter-electrode gap during leveling process in counter-rotating electrochemical machining. Chin J Aeronaut 32(11):2557–2565. https://doi.org/10.1016/j.cja.2019.08.022

16. Clifton D, Mount AR, Alder GM, Jardine D (2002) Ultrasonic measurement of the inter-electrode gap in electrochemical machining. Int J Mach Tools Manuf 42:1259–1267. https://doi.org/10.1016/S0890-6955(02)00041-X

17. Yun NZ (1989) Investigation on application of electrochemical contour evolution machining. In: Proceedings of the ISEM-9 143-145

18. Wei B, Rajurkar KP (1990) Accuracy and dynamics of 3-dimensional numerical control electrochemical machining (NC-ECM). In: Proc of winter annual meeting of the ASME PED, vol 45, pp 33–45

19. Kozak J, Rajurkar KP (1998) Sculptured Surface Finishing NC-electrochemical machining with ball-end electrode. Adv Tech Mach Equip 22:53–74

20. Jiawen X, Naizhang Y, Yangxin T, Rajurkar KP (2005) The modeling of NC-electrochemical contour evolution machining using a rotary tool-cathode. J Mat Proc Tech 159:272–277. https://doi.org/10.1016/j.jmatprotec.2004.05.013

21. Yong L, Yunfei Z, Guang Y, Liangqiang P (2003) Localized electrochemical micromachining with gap control. Sens Actuators A 108:144–148. https://doi.org/10.1016/S0924-4247(03)00371-6

22. Kurita T, Chikamori K, Hattori KS, M (2006) A study of three-dimensional shape machining with an ECM system. Int J Mach Tools Manuf 46:1311–1318. https://doi.org/10.1016/j.ijmachtools.2005.10.013

23. Labib AW, Keasberry VJ, Atkinson J, Frost HW (2011) Towards next-generation electrochemical machining controllers: a fuzzy logic control approach to ECM. Expert Syst Appl 38:7486–7493. https://doi.org/10.1016/j.eswa.2010.12.074

24. Liu S, Thangaraj M, Moiduddin K, Al-Ahmari AM (2022) Influence of adaptive gap control mechanism and tool electrodes on machining titanium (Ti-6Al-4V) alloy in EDM process. Materials 15(2):513. https://doi.org/10.3390/ma15020513

25. Özerkan HB, Çoğun C (2020) Electrochemical small diameter deep hole drilling of powder metal steel. Trans FAMENA 44:47–58. https://doi.org/10.21278/TOF.444007919